Acta Neuropathol (2008) 115:175–183
DOI 10.1007/s00401-007-0330-6

ORIGINAL PAPER

Tracing of temporo-entorhinal connections in the human brain: cognitively impaired argyrophilic grain disease cases show dendritic alterations but no axonal disconnection of temporo-entorhinal association neurons

Dietmar Rudolf Thal · Estibaliz Capetillo-Zarate · Ralf A. Galuske

Received: 15 October 2007 / Revised: 30 November 2007 / Accepted: 2 December 2007 / Published online: 14 December 2007

Abstract Argyrophilic grain disease (AGD), a neurodegenerative disorder, is often associated with mild to moderate Alzheimer's disease (AD)-related pathology. The development of dementia in AGD is associated with the extent of coexisting AD-related pathology. Therefore, the question arises whether the degenerative changes in the neuronal network of demented AGD-patients represent a distinct pattern or show similar changes of disconnection as considered for AD. We were able to apply DiI-tracing in two human autopsy cases with mild AD-related pathology (controls), in one AD-patient, in one non-demented patient with advanced AD-related pathology, and in three cognitively impaired AGD-patients. DiI-crystals were injected into the entorhinal cortex. Pyramidal neurons of layers III and V of the adjacent temporal neocortex (area 35) were retrogradely marked with the tracer and analyzed. The AD case did not exhibit any retrogradely labeled neurons in the temporal neocortex. In the non-demented case with advanced AD-related pathology, the number of traced neurons was reduced as compared to that in the two controls and in the three AGD cases. In contrast, all three cognitively impaired AGD cases exhibited labeled pyramidal neurons in area 35 in an almost similar number as in the controls. However, alterations in the dendritic tree were observed in the AGD cases. These results show the existence of temporo-entorhinal connections in the adult human brain similar to those reported in animal models. Furthermore, the present study based on seven cases is the first attempt to study changes in the neuronal network in a human tauopathy with targeted axonal tracing techniques. Our findings in three cognitively impaired AGD cases suggest that AGD-related dementia constitutes a distinct disorder with a characteristic pattern of degeneration in the neuronal network.

Keywords Alzheimer's disease · Argyrophilic grain disease · Tracing · Association neurons · Neuronal connectivity

D. R. Thal (✉)
Department of Pathology, Laboratory of Neuropathology, University of Ulm, Albert-Einstein-Allee 11, 89081 Ulm, Germany
e-mail: dietmar.thal@uni-ulm.de

D. R. Thal · E. Capetillo-Zarate
Department of Neuropathology, University of Bonn, Bonn, Germany

R. A. Galuske
Department of Biology, Technical University Darmstadt, Darmstadt, Germany

Present Address:
E. Capetillo-Zarate
Department of Neurology and Neuroscience, Weill Medical College of Cornell University, New York, NY 10021, USA

Introduction

Alzheimer's disease (AD) and argyrophilic grain disease (AGD) are dementing disorders, which lead to degeneration of the medial temporal lobe [2, 4, 5, 29]. Although both disorders are tauopathies they differ in the type of tau-lesions and in the types of neurons affected [4]. Neurofibrillary tangles (NFTs), neuropil threads, neuritic plaques as well as neuronal loss prevail in AD, whereas argyrophilic grains, oligodendroglial coiled bodies, ballooned neurons and tau-positive astrocytes are hallmarks of AGD [3, 4, 41]. The

role of AGD for the development of dementia is controversially discussed. Some reports showed patients in whom dementia was explained by AGD although low levels of AD-related changes also prevailed [4, 31, 38]. On the other hand, dementia in AGD-patients was more frequently seen in association with moderate to severe AD-related changes than in those with less severe AD-related pathology [22, 36]. Therefore, the question arises whether AGD is a distinct type of dementia or AD with additive pathological changes [22].

We were able to apply DiI-tracing in seven autopsy cases with mild AD-related pathology, with moderate to severe AD-related pathology, AD, and with AGD-related cognitive deficits. Here, we studied the pattern of alterations in temporo-entorhinal association neurons in AGD. Temporo-entorhinal association neurons connect two regions, which are affected early in the course of AD and AGD, and in close anatomical proximity. These fibers have been described in monkeys [19, 43]. To our knowledge, their existence has not been demonstrated in the adult human brain until now. Only single neurons have been traced in fetal human brain [14]. Here, we were able to show this fiber tract in the human adult brain and to study its involvement in AGD.

Materials and methods

Clinical and neuropathological characterization

Seven brains from human autopsy cases with a postmortem-interval ranging from 6 to 23 h (mean 12 h) were used for DiI-tracing (Table 1). Selection criteria were postmortem-intervals of <24 h and the possibility to dissect the entire left medial temporal lobe for tracing from the unfixed brain as previously published [12]. Demented as well as non-demented patients had been examined 1–4 weeks prior to death according to standardized protocols used for routine clinical and neurological examination of patients upon admission to the hospital. Protocols included the assessment of cognitive function and recorded the ability to care for and dress oneself, eating habits, bladder and bowel continence, speech patterns, writing and reading skills, short-term and long-term memory, and the orientation within the hospital setting. These data were used to retrospectively apply the clinical dementia rating (CDR) test [18] as well as the global deterioration scale (GDS) test [30]. Using these data it was examined whether individuals clinically fulfilled the DSM-IV criteria for dementia [1] or not. AD was diagnosed when dementia was observed and AD-related pathology at autopsy fulfilled recommended criteria for the diagnosis of AD [37].

Except for the left medial temporal lobe, which was used for DiI-tracing, brains were fixed in a 4% aqueous formaldehyde solution for at least 3 weeks. Blocks of the right MTL were taken at the levels of the (1) anterior limit of the dentate gyrus, (2) lateral geniculate body, and (3) posterior limit of the dentate gyrus [20]. The tissue blocks were embedded in polyethylene glycol (PEG) [6] and in paraffin. The PEG-blocks were microtomed at 100 µm, whereas the paraffin sections were cut at 10 µm.

Neurofibrillary changes and argyrophilic grains were detected using the Gallyas-silver-staining method [6, 21]. Abnormal phosphorylated tau-protein was recognized with a monoclonal antibody (AT-8; Innogenetics; Belgium; 1/1,000). The presence of amyloid deposits was assessed using the Campbell–Switzer silver impregnation method [6, 21] and/or using immunohistochemistry with an antibody directed against $A\beta_{17-24}$ (4G8; Signet; Dedham; USA; 1/5,000; formic acid pretreatment). For topographical orientation and neuropathological diagnosis, serial paraffin and PEG sections were stained with aldehydefuchsin-Darrow-

Table 1 List of cases with neuropathological and clinical results and type of neurodegeneration as determined by DiI-tracing

Case number	Age	Gender	NFT (Braak)-stage	CERAD-score	Aβ-phase	CDR	GDS	Diagnosis	Type of neurodegeneration	Number of traced association neuron in area 35	PMI
1	91	F	2	0	1	0	1	ADRP	0	18	6
2	90	F	3	0	1	0	1	ADRP	0	12	11.5
3	77	M	3	A	2	0.5	3	AGD	AGD-dendritic degeneration	13	12
4	80	F	2	A	3	1	6	AGD	AGD-dendritic degeneration	8	12
5	81	M	2	A	3	2	6	AGD	AGD-dendritic degeneration	12	9
6	87	F	4	B	3	3	6	AD	AD-disconnection	0	23
7	67	M	4	A	4	0	1	Severe ADRP	AD-disconnection	5	12.5

F female, *M* male, *AD* Alzheimer's disease, *ADRP* non-demented with AD-related pathology, *AGD* argyrophilic grain disease, 0 no neurodegeneration, and *PMI* postmortem-interval (h)

NFT (Braak)-stage according to [5], CERAD-score according to [24], Aβ-phase according to [35], clinical dementia rating score (CDR) according to [25], and global deterioration scale (GDS) according to [30]

red for lipofuscin pigment and Nissl material. Cyto- and pigmentoarchitectural parcellations of the entorhinal layers were performed according to Braak and Braak [7]. Diagnosis of the stages in the development of neurofibrillary changes (Braak-stage) was performed in accordance with published criteria [5, 37]. The frequency of neuritic plaques (CERAD-score) was assessed as recommended by Mirra et al. [24] using Gallyas-stained sections. For the Braak staging and CERAD-scores additional sections from the occipital cortex, including the primary visual cortex, were analyzed. For staging of Aβ-pathology, we used the recently described four phases of β-amyloidosis in the MTL [34]. This hierarchy based procedure enables us to explore the expansion of Aβ-deposition into additional brain regions [34, 35]. Phase 1 represents Aβ-deposits that are restricted to the temporal neocortex. Phase 2 is characterized by additional Aβ-plaques in the entorhinal cortex and/or in the subiculum-CA1 region. The third phase of β-amyloidosis exhibits additional Aβ-plaques in the outer zone of the molecular layer of the fascia dentata, subpial band-like amyloid and/or the presubicular "lake-like" amyloid. The presence of additional Aβ-plaques in CA4 and/or the pre-α-layer of the entorhinal cortex marks the fourth and final phase of Aβ-deposition.

Diagnosis of AGD was based on the detection of argyrophilic grains in the Gallyas-stained sections and on the presence of coiled bodies, tau-positive astrocytes, and ballooned neurons exhibiting abnormal tau protein [4, 41].

Tissue preparation and DiI-tracing

The unfixed brain was cut into frontal slabs of approximately 10 mm thickness. At the level of the entorhinal region and the uncus formation, the left medial temporal lobe including the hippocampal formation, entorhinal region, and adjacent temporal neocortex (areas 35 and 36) was cut and immediately fixed in 0.1 M phosphate buffered saline (PBS) (pH 7.4) containing 2.6% paraformaldehyde (PFA), 0.8% iodoacetic acid, 0.8% sodiumperiodate, and 0.1 M D-L Lysine for 5 days as previously published [12]. After 5 days, a single DiI-crystal (Molecular Probes, Eugene, OR, USA) was implanted into the entorhinal layers (Fig. 1) as described previously [9, 12]. One DiI-crystal was placed into each side of the sample to ensure tracing of neurons in the entire sample. In order to ensure that the injection sizes were of similar extent in all cases, individual dye crystals were glued to the tip of a glass capillary using ethanol and then measured under a microscope before implantation. For injection, dye crystals exhibiting a diameter of about 500 µm were selected. Postmortem tracing with DiI allows a precise Golgi-like tracing of neurons in fixed tissues with a quality similar to that of in vivo tracing techniques such as biotinylated dextrane amines or rhodamine labeled latex microspheres in combination with intracellular filling with Lucifer Yellow [11]. After incubation in 2.0% phosphate buffered PFA for at least 12 months at 37°C, 100 µm thick coronal vibratome sections were cut. Sections were mounted in TBS for microscopic analysis.

Microscopic and quantitative analysis

Every third section of the medial temporal lobe samples of each human autopsy case was examined using a Leica DMLB fluorescence microscope. The distance between the tracer application site in the entorhinal cortex and area 35 was approximately 6–9.5 mm. Ten sections of the level of the implanted tracer were used to quantify the number of traced pyramidal neurons in layer III and layer V of the temporal neocortex in Brodmann area 35. This part of the neocortex adjoins the entorhinal region (area 28). Association fibers connect both regions. The transentorhinal region sets the boundary between these regions (Fig. 1). In cases where no labeled neurons were detected, it was determined whether at least labeled neurites could be found. In the event that retrogradely labeled neurons were present, the number of stained pyramidal neurons in area 35 was assessed in ten subsequent sections cut at a thickness of 100 µm. Thus, the number of neurons in a 1-mm-thick slab of the area 35 was determined. Then, the dendritic tree of labeled neurons was investigated. Primary and secondary branches of the dendritic tree were analyzed. A laser scanning confocal microscope (Leica TCS NT, Leica, Bensheim, Germany) was used. Stacks of 2D images were superimposed digitally using the Image J Imaging Processing and Analysis software (NIH, Bethesda, MD, USA), and 3D data sets were generated for the visualization of neurons with their entire dendritic tree.

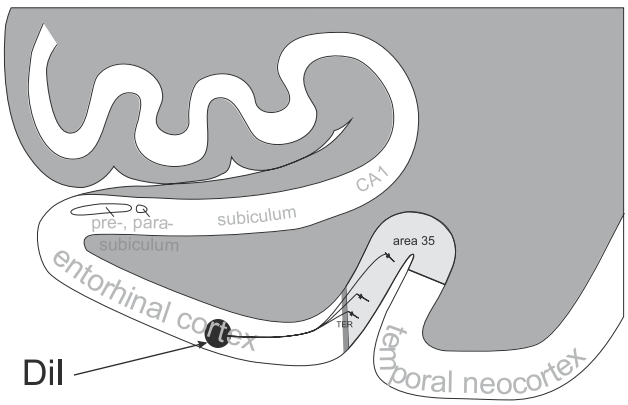

Fig. 1 Schematic representation of postmortem tracing with DiI. DiI-crystals (*arrow*) were injected into the upper layers of the entorhinal cortex (area 28). Pyramidal neurons of the adjacent temporal cortex of area 35 (cortex in the *boxed area*) were retrogradely traced in the control cases. *TER* transentorhinal region

Results

DiI application into the entorhinal cortex of the two non-demented patients with low levels of AD-related pathology (controls) marked a high number of neurites projecting into area 35 of the temporal cortex as well as 12–18 retrogradely labeled pyramidal neurons in layers III and V in a 1-mm-thick slab of the area 35 (Figs. 2, 3; Table 1). The number of neurons per section varied between 0 and 4. The neurons were, thereby, organized in clusters of 2–3 in one section (Fig. 2b, c). These neurons showed a symmetric dendritic tree with basal dendrites of similar size (Fig. 3). The proximal parts of the basal dendrites showed larger calibers than the distal parts. Neurons from other parts of the temporal cortex were not traced.

The cognitively impaired AGD cases with moderate levels of AD-related pathology exhibited 8–13 retrogradely traced neurons in a 1-mm-thick slab of area 35 (Fig. 2, Table 1). At higher magnification, these neurons displayed alterations of their dendritic tree. Although the dendritic tree exhibited a symmetric pattern, a high number of basal dendrites of layers III and V pyramidal neurons showed proximal caliber thinning not seen in controls (Fig. 3). The dendritic spines were more prominent in the AGD cases than in the two control cases and the dendrites exhibited a "clumsy" pattern. The existence of "clumsy" structures in contact with the branches of the dendrites was confirmed by analyzing 3D-reconstructions of the dendrite with the confocal laser scan microscope excluding dendritic beading as well as artificial beading (Fig. 3g–k). The morphology of the "clumsy" spines was similar to that of abnormal phosphorylated tau-protein in argyrophilic grain disease-affected neurons (Figs. 4c, 5).

In the non-demented Braak-stage-IV Aβ-phase-4 case lacking AGD-pathology, only five neurons were retrogradely labeled in a 1-mm-thick slab of the area 35. The dendrites of these neurons did not exhibit "clumsy" changes as seen in the AGD cases (Fig. 3f). In the AD cases there was no retrograde tracing of pyramidal neurons in the temporal cortex of area 35. However, the sparse presence of individually stained neurites indicated that the tracing had in principle been successful (Figs. 2, 3c; Table 1).

Based on these results, we distinguished different types of neurodegeneration as provided in Table 1: (1) no neurodegeneration, i.e., neurons traced in area 35 exhibit a regular dendritic tree; (2) dendritic degeneration, i.e., neurons with traced basal dendrites showing proximal caliber thinning and "clumsy" spines in area 35; and (3) neuronal disconnection, i.e., more than 50% reduction of the traced association neurons in the association cortex.

The Gallyas-silver-staining revealed a high number of NFTs in area 35 of the Braak-stage-IV cases while only single NFTs were found in control and AGD cases with lower

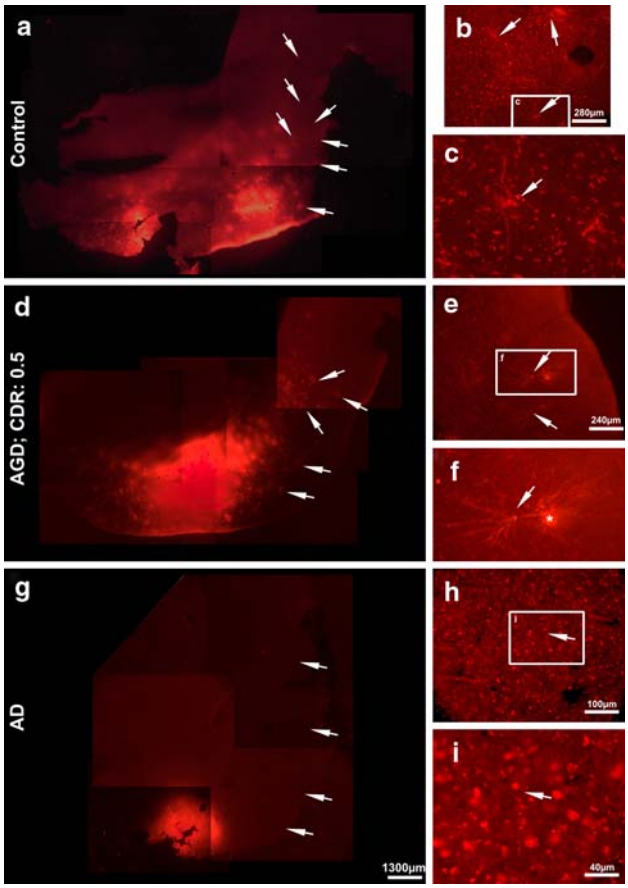

Fig. 2 Disconnection of the entorhinal–temporal association fiber tract in an AD case but not in cognitively impaired AGD and control cases. **a** DiI-tracing of entorhinal–temporal connections in the control case (case No. 2) exhibited DiI-labeled structures in area 35 of the temporal neocortex (*arrows*). **b** Detailed view into the temporal cortex of area 35 of the control case. Here, a group of three neurons (*arrows*) was labeled. One neuron (*boxed area*) is enlarged in **c**. The cell soma and the basal dendrites were traced (*arrow*). **d** A similar pattern of traced neurons was seen in the cognitively impaired AGD case (*arrows*; case No. 3). **e** The detailed view into area 35 showed a cluster of two neurons (*arrows*). One neuron (*boxed area*) is enlarged in **f** showing the soma with the dendritic tree (*arrow*). Artificially stained material was in contact with the neuron and is indicated by an *asterisk*. **g** No DiI-labeling of association fibers in the temporal cortex of the AD case (*arrows*; case No. 6). **h** Only single neurites (*arrow* in **h** and **i**) were detectable in the entorhinal cortex (*boxed area*) and are enlarged in **i** and Fig. 3c. *Calibration bar* **g** valid for **a**, **d**, **and g**; and **h** valid for **c**, **f**, and **h**

Braak-stages (II and III) (Fig. 4). The Gallyas-stained temporal neocortex of both Braak-stage-III cases is depicted in Fig. 4e, f showing only single NFTs, whereas numerous NFTs were found in the Braak-stage-IV case (Fig. 4g). The three AGD cases revealed grains (Fig. 4b), coiled bodies, tau-positive astrocytes, neurons (Fig. 4c), and ballooned neurons in sections stained for abnormal phosphorylated tau-protein. Only a few grains and coiled bodies were seen in Gallyas-silver-stained sections. Similarly, the two cases with neuronal disconnection exhibited higher phases of Aβ-deposition than cases with traceable neurons in area 35.

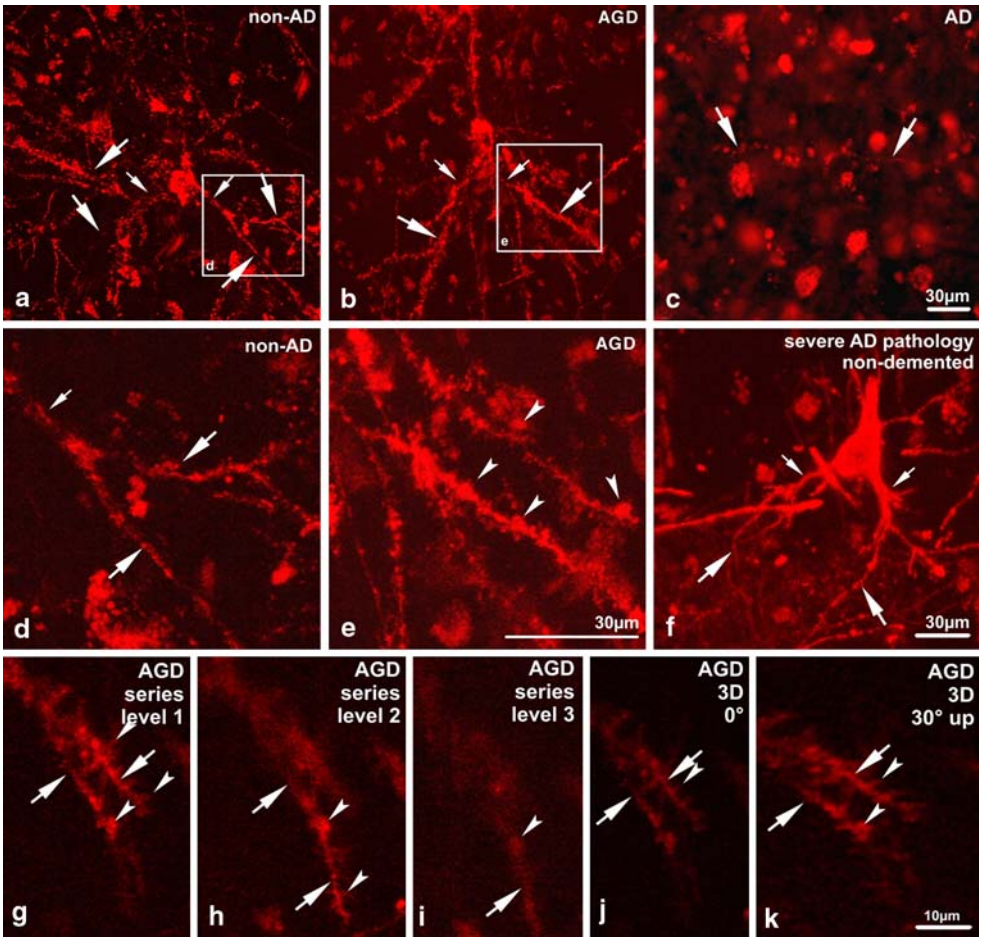

Fig. 3 Degeneration of dendrites in traced temporal layer III pyramidal neurons of area 35 of the temporal cortex. To analyze the integrity and structure of the dendrites stacks of ten images obtained by confocal laser scan microscopy in ~10 µm distance were superimposed in a Z-project or analyzed in a 3D-project using the image J software. **a** Z-project. The pyramidal neurons of the non-demented control case (case No. 2) showed a symmetric dendritic tree with branching basal dendrites. The distal branches (*large arrows*) were smaller than the proximal ones (*small arrows*). The *boxed area* in **a** is enlarged in **d**. At high power magnification, only small spine-like structures were seen (*arrows* in **d**). **b** Z-project. The cognitively impaired AGD case (case No. 3) showed neurons with thin proximal basal dendrites (*small arrows*). The distal dendrites often appeared to have a similar or larger diameter (*large arrows*). High power laser-scan microscopy (*boxed area e*, enlarged in **e**) revealed prominent clumsy spines on the basal dendrites (*arrowheads* in **e**). **c** Fluorescence microscopy. The AD case No. 6 did not show labeling of neurons. Only few single neurites (*arrows*) were traced in the entorhinal cortex near the tracer application site indicating severe degeneration of the local neuronal network. **f** Z-Project. A surviving association neuron in the temporal neocortex of the non-demented case with severe AD-related pathology (case No. 7) showed basal dendrites without clumsy spines in a pattern similar to non-AD cases with mild AD-related pathology **a, d**. The proximal dendrites (*small arrows*) were thicker than the distal ones (*large arrows*). **g–i** Confocal images at three different levels indicate that there is no obvious dendritic beading (*arrows* in **g–i**). Three dimensional reconstruction presented in two different perspectives confirming the absence of dendritic beading (*arrows* in **j, k**). Clumsy dendritic spines were identified (*arrowheads* in **g–i**) and confirmed by 3D reconstruction (*arrowheads* in **j, k**). *Calibration bar* **c** valid for **a–c**; **e** valid for **d** and **e**; and **k** valid for **g–k**

Moreover, the cases with dendritic degeneration had higher phases of Aβ-deposition than the controls with only mild AD-related pathology (Table 1).

Discussion

DiI-tracing into the entorhinal cortex demonstrated that temporo-entorhinal connections exist in the adult human brain similar to that described in animals earlier [19, 43]. These association fibers arise from pyramidal cells in layers III and V of the area 35. As reported for other interhemispheric connections [12, 32], temporo-entorhinal connections also arise from small clusters of temporal neurons presumably representing the modular architecture of the cerebral cortex. The distribution of these clusters varied among different sections of the same individual and explains the variation of labeled neurons between individual cases. Association fibers from other parts of the temporal cortex have not been observed.

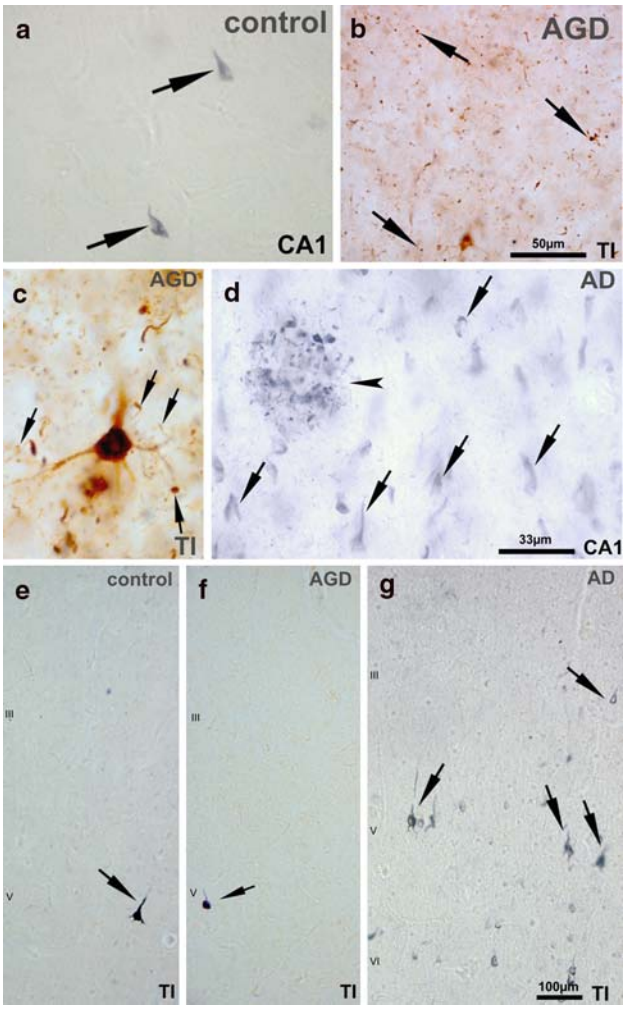

Fig. 4 **a** The Gallyas-silver-stained section of the control case No. 2 with Braak-stage-III confirmed the presence of single NFTs (*arrows*) in CA1. **b** Using an antibody, directed against abnormal tau-protein, argyrophilic grains (*arrows*) were predominant in the temporal neocortex (area 35) of the AGD case No. 3. **c** The Z-project of three images of ~10 µm focus distance showed a neuron of the same AGD case exhibiting abnormal phosphorylated tau-protein with clumsy, grain-like structures in the basal dendrites (*arrows*). **d** The AD case (case No. 6) exhibited high numbers of Gallyas-positive NFTs (*arrows*) and a neuritic plaque (*arrowhead*) in CA1. **e, f** In the temporal cortex of area 35 in the control (**e**; case No. 2) and in the AGD-brain (**f**; case No. 3) only single neurons of layer V contained Gallyas-positive neurofibrillary material (*arrows*). **g** In the AD case a large number of Gallyas-positive NFTs (*arrows*) were seen in layers III, V, and VI as compatible with Braak-stage-IV and higher. *TI* temporal neocortex of area 35 and *CA1* Ammon's horn sector CA1. *Calibration bar* **b** valid for **a** and **b**; **d** valid for **c** and **d**; and **g** valid for **e–g**

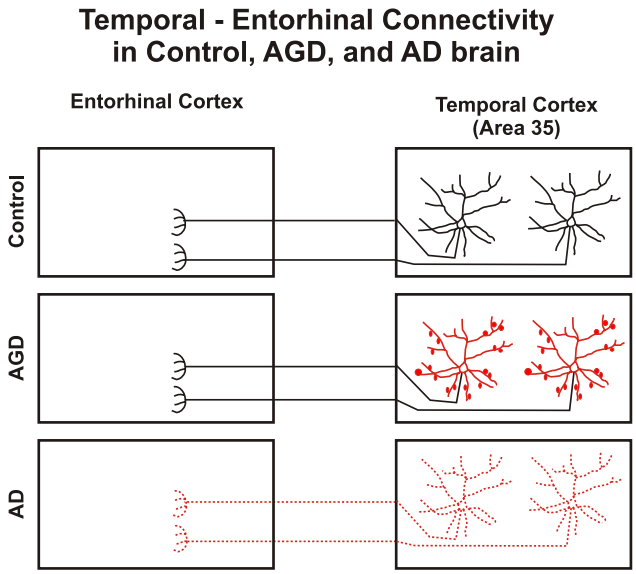

Fig. 5 Schematic representation of temporal–entorhinal connectivity in control, AGD and AD brain. In aged controls with minimal AD-related changes temporal and entorhinal cortices are connected. Typical pyramidal neurons project into the entorhinal cortex. In AGD temporal and entorhinal cortices are connected but the projecting pyramidal neurons display dendritic alterations (marked in *red*). Axonal disconnection is seen in AD. Neurons, which once were connected, are no longer detectable with DiI-tracing (scattered neurons marked in *red*). The *red-labeled* parts of the association neurons were obviously altered in AGD and AD, respectively. Disconnection in AD can most likely be explained as the result of neuronal loss [5, 13, 15, 26, 33]

Within seven cases examined in the present study using postmortem tracing with DiI, a disconnection of association fibers between the entorhinal and the adjacent temporal neocortex was seen in an AD case and in one non-demented case with Braak-stage-IV AD-related pathology. By contrast, all cognitively impaired patients with AGD-pathology did not exhibit obvious disconnection between the entorhinal and the temporal neocortex. However, they displayed dendritic tree abnormalities as compared to the two non-demented cases with mild AD-related pathology lacking AGD and to the non-demented case with severe AD-related pathology.

To our knowledge, this is the first report showing disconnection in an AD brain with a tracing technique and demonstrating intact connectivity in cognitively impaired patients with AGD. Only dendritic alterations were found in AGD. However, one obvious limitation of this study is its small sample size. Given the manifold prerequisites for successful postmortem tracing [12], i.e., (1) postmortem-interval <24 h, (2) preparation and fixation for tracing at autopsy, and (3) a 10-mm-thick piece of the medial temporal lobe received from research cases not included into a specific brain bank protocol, the number of available cases for such tracing experiments was very low.

DiI-tracing is a postmortem tracing technique, which has already been successfully used to study connections in the human autopsy brain with a postmortem delay up to and including 24 h [12, 14, 27, 32]. This technique labels all cells retrogradely and anterogradely in a Golgi-like pattern by diffusion in membrane structures, which are in touch with the tracer [16, 17]. In animals, it has been shown that this technique labels all processes of a stained neuron as if

it is marked with a rhodamine tracer [11] and that the pattern of the traced neurons is similar to that detected by in vivo tracing with biotinylated dextrane [9]. By this, the tracing method leads to valid results in postmortem tissue when applied shortly after death as done in the cases studied here.

The reduction of the number of tracer-labeled association neurons in area 35 in the AD case and in the non-demented Braak-stage-IV case indicates that there was a disconnection between the temporal cortex of area 35 and the entorhinal cortex. Since single neurites and neurons were marked, the tracing was considered to be successful. Therefore, insufficient tracing is unlikely to explain the reduction of connectivity. Our finding of disconnection in the temporal cortex is in line with the decrease of axonal transport reported in the temporal neocortex of AD-patients [10]. Since neurofibrillary pathology and neuronal loss start in the transentorhinal–entorhinal cortex and subsequently involve the basal temporal neocortex in Braak-stage-IV [5, 13], the onset of disconnection in this early affected part of the brain may be explained by the affection of the local pyramidal neurons by neurofibrillary pathology and neuronal loss [5, 13, 33]. In the Braak-stage-II and III cases studied here, there was only mild affection of single neurons carrying NFTs in the temporal association cortex explaining the preservation of connectivity in the non-demented and AGD cases. Based on the results of clinico-pathological correlation studies, Hof et al. [15, 26] suggested that neuronal disconnection is involved in the development of cognitive decline in AD. The absence of traceable temporo-entorhinal connections in our AD case supports this hypothesis. The presence of multiple NFTs in the temporal neocortex of the Braak-stage-IV AD case further indicates severe damage of the neurons in the area 35.

By contrast, anatomical disconnection is not a prerequisite for developing dementia in all tauopathies. All of the three cognitively impaired or demented AGD cases studied here exhibited no substantial anatomical disconnection. Neurons in area 35 were traced in an almost similar quantity as in the two non-demented elderly brains with mild AD-related pathology. Moreover, neuronal loss or brain tissue loss responsible for tissue shrinkage is often not detectable in AGD cases [41], which has been suspected to underlie the AD-related disconnection [15]. However, the pattern of the dendritic tree pathology in AGD differed from that in the non-demented non-AGD cases. In the demented AGD cases, proximal thinning of basal dendrites as well as clumsy spines was seen but these changes were absent in non-AGD cases. Dendritic beading, which may also explain a "clumsy" pattern of the dendrites due to excitotoxic events [28], could be excluded by 3D-reconstruction of serial scans with the laser scan microscope through the 100-µm-thick section. Even though the connectivity seemed to be intact as indicated by retrogradely labeled neurons, the observed changes in the morphology of dendrites in AGD cases may thus lead to functional deficits underlying dementia. This pattern of predominant dendritic changes in AGD reflects the pattern of tau and argyrophilic pathology in this disease. Only grains and glial inclusions are argyrophilic in AGD [8]. Abnormal phosphorylated tau-protein, however, occurs in neurons but it shows in addition to a somatic distribution, a characteristic staining of spines often exhibiting a clumsy, grain-like appearance [39].

Comparison of the three cognitively impaired AGD-patients with the patients with severe AD-related pathology or AD points to distinct differences in the pattern of neurodegeneration between AGD and AD. The AD-type of dementia is suggested to receive its major morphological correlation by anatomical disconnection as reported earlier [15], whereas AGD-related cognitive impairment appears to be due to dendritic degeneration preserving the axonal connections (Fig. 5). The lack of similar AGD-like dendritic alterations in non-disconnected association neurons of the case with severe AD-related pathology further supports that distinct dendritic alterations occurred in the AGD cases. Recently, others and we have shown that demented AGD cases have more severe additional AD-related pathology than non-demented AGD cases [22, 36]. Josephs et al. [22] hypothesized that AGD may not be a distinct disorder but AD with additive pathology. The existence of our three cognitively impaired cases with AGD showing a pattern of alterations in the neuronal network different from that seen in an AD case argues against this hypothesis. Thus, our tracing study supports the concept of other authors [4, 23, 31] that AGD is a distinct neurodegenerative disorder. However, the coexistence of AGD and AD pathologies in the brain will lead to additive effects of both degenerative mechanisms lowering the threshold for developing dementia for each of the two pathologies as reported earlier [36].

The extent to which Aβ-aggregates, which were seen in all of our demented AGD cases studied here, induce dendritic changes in AGD-brains, is still debatable. Animal experiments showing dendritic alterations induced by Aβ-aggregates [9, 42, 44] are in support of this notion. The coexistence of Aβ-deposits in the brain of cognitively impaired AGD cases can be interpreted along the same line [22, 36, 40]. However, further studies are required to address the contribution of Aβ to AGD-like neurodegeneration.

In summary, this report of seven cases shows that dendritic alteration but not anatomical disconnection characterizes AGD. This type of neurodegeneration is opposed by the concept of anatomical disconnection in AD [15], which is supported by our tracing results in cases with advanced AD-related pathology and AD (Fig. 5).

Acknowledgments The authors gratefully acknowledge the technical assistance of N. Kolosnjaji and H. U. Klatt. This study was supported by the University of Bonn (BONFOR-Grant No. O-154.0041) and by the DFG (Grant No. TH624/4-2) (D. R. T.). Human autopsy tissue was studied according to the German law for using human tissue in agreement with the vote of the Local Ethical Committee of the Universities of Bonn and Ulm.

References

1. American Psychiatric Association (1994) Diagnostic and statistical manual of mental disorders. American Psychiatric Association, Washington
2. Arnold SE, Hyman BT, Flory J, Damasio AR, Van Hoesen GW (1991) The topographical and neuroanatomical distribution of neurofibrillary tangles and neuritic plaques in the cerebral cortex of patients with Alzheimer's disease. Cereb Cortex 1:103–116
3. Botez G, Probst A, Ipsen S, Tolnay M (1999) Astrocytes expressing hyperphosphorylated tau protein without glial fibrillary tangles in argyrophilic grain disease. Acta Neuropathol (Berl) 98:251–256
4. Braak H, Braak E. (1987) Argyrophilic grains: characteristic pathology of cerebral cortex in cases of adult onset dementia without Alzheimer changes. Neurosci Lett 76:124–127
5. Braak H, Braak E (1991) Neuropathological staging of Alzheimer-related changes. Acta Neuropathol 82:239–259
6. Braak H, Braak E (1991) Demonstration of amyloid deposits and neurofibrillary changes in whole brain sections. Brain Pathol 1:213–216
7. Braak H, Braak E (1992) The human entorhinal cortex: normal morphology and lamina-specific pathology in various diseases. Neurosci Res 15:6–31
8. Braak H, Braak E (1998) Argyrophilic grain disease: frequency of occurrence in different age categories and neuropathological diagnostic criteria. J Neural Transm 105:801–819
9. Capetillo-Zarate E, Staufenbiel M, Abramowski D, Haass C, Escher A, Stadelmann C, Yamaguchi H, Wiestler OD, Thal DR (2006) Selective vulnerability of different types of commissural neurons for amyloid beta-protein induced neurodegeneration in APP23 mice correlates with dendritic tree morphology. Brain 129:2992–3005
10. Dai J, Buijs RM, Kamphorst W, Swaab DF (2002) Impaired axonal transport of cortical neurons in Alzheimer's disease is associated with neuropathological changes. Brain Res 948:138–144
11. Galuske RA, Singer W (1996) The origin and topography of long-range intrinsic projections in cat visual cortex: a developmental study. Cereb Cortex 6:417–430
12. Galuske RA, Schlote W, Bratzke H, Singer W (2000) Interhemispheric asymmetries of the modular structure in human temporal cortex. Science 289:1946–1949
13. Gomez-Isla T, Price JL, McKeel DW Jr, Morris JC, Growdon JH, Hyman BT (1996) Profound loss of layer II entorhinal cortex neurons occurs in very mild Alzheimer's disease. J Neurosci 16:4491–4500
14. Hevner RF, Kinney HC (1996) Reciprocal entorhinal–hippocampal connections established by human fetal midgestation. J Comp Neurol 372:384–394
15. Hof PR, Bouras C, Constantinidis J, Morrison JH (1990) Selective disconnection of specific visual association pathways in cases of Alzheimer's disease presenting with Balint's syndrome. J Neuropathol Exp Neurol 49:168–184
16. Honig MG, Hume RI (1989) Dil and diO: versatile fluorescent dyes for neuronal labeling and pathway tracing. Trends Neurosci 12:333–335, 340–331
17. Honig MG, Hume RI (1989) Carbocyanine dyes. Novel markers for labelling neurons. Trends Neurosci 12:336–338
18. Hughes CP, Berg L, Danziger WL, Coben LA, Martin RL (1982) A new clinical scale for the staging of dementia. Br J Psychiatry 140:566–572
19. Insausti R, Amaral DG, Cowan WM (1987) The entorhinal cortex of the monkey: II. cortical afferents. J Comp Neurol 264:356–395
20. Insausti R, Amaral DG (2004) Hippocampal formation. In: Paxinos G, Mai JK (eds) The human nervous system. Elsevier, London, pp 872–914
21. Iqbal K, Braak H, Braak E, Grundke-Iqbal I (1993) Silver labeling of Alzheimer neurofibrillary changes and brain beta-amyloid. J Histotechnol 16:335–342
22. Josephs KA, Whitwell JL, Parisi JE, Knopman DS, Boeve BF, Geda YE, Jack CR Jr, Petersen RC, Dickson DW (2006) Argyrophilic grains: a distinct disease or an additive pathology? Neurobiol Aging
23. Martinez-Lage P, Munoz DG (1997) Prevalence and disease associations of argyrophilic grains of Braak. J Neuropathol Exp Neurol 56:157–164
24. Mirra SS, Heyman A, McKeel D, Sumi SM, Crain BJ, Brownlee LM, Vogel FS, Hughes JP, van Belle G, Berg L (1991) The consortium to establish a registry for Alzheimer's disease (CERAD). Part II. Standardization of the neuropathologic assessment of Alzheimer's disease. Neurology 41:479–486
25. Morris JC (1993) The clinical dementia rating (CDR): current version and scoring rules. Neurology 43:2412–2414
26. Morrison JH, Hof PR (1997) Life and death of neurons in the aging brain. Science 278:412–419
27. Mufson EJ, Brady DR, Kordower JH (1990) Tracing neuronal connections in postmortem human hippocampal complex with the carbocyanine dye DiI. Neurobiol Aging 11:649–653
28. Oliva AA Jr, Lam TT, Swann JW (2002) Distally directed dendrotoxicity induced by kainic acid in hippocampal interneurons of green fluorescent protein-expressing transgenic mice. J Neurosci 22:8052–8062
29. Price JL, Davis PB, Morris JC, White DL (1991) The distribution of tangles, plaques and related immunohistochemical markers in healthy aging and Alzheimer's disease. Neurobiol Aging 12:295–312
30. Reisberg B, Ferris SH, de Leon MJ, Crook T (1988) Global deterioration scale (GDS). Psychopharmacol Bull 24:661–663
31. Saito Y, Ruberu NN, Sawabe M, Arai T, Tanaka N, Kakuta Y, Yamanouchi H, Murayama S (2004) Staging of argyrophilic grains: an age-associated tauopathy. J Neuropathol Exp Neurol 63:911–918
32. Tardif E, Probst A, Clarke S (2007) Laminar specificity of intrinsic connections in Broca's area. Cereb Cortex 17:2949–2960
33. Terry RD, Peck A, DeTeresa R, Schechter R, Horoupian DS (1981) Some morphometric aspects of the brain in senile dementia of the Alzheimer type. Ann Neurol 10:184–192
34. Thal DR, Rüb U, Schultz C, Sassin I, Ghebremedhin E, Del Tredici K, Braak E, Braak H (2000) Sequence of Abeta-protein deposition in the human medial temporal lobe. J Neuropathol Exp Neurol 59:733–748
35. Thal DR, Rüb U, Orantes M, Braak H (2002) Phases of Abeta-deposition in the human brain and its relevance for the development of AD. Neurology 58:1791–1800
36. Thal DR, Schultz C, Botez G, Del Tredici K, Mrak RE, Griffin WS, Wiestler OD, Braak H, Ghebremedhin E (2005) The impact of argyrophilic grain disease on the development of dementia and its relationship to concurrent Alzheimer's disease-related pathology. Neuropathol Appl Neurobiol 31:270–279
37. The National Institute on Aging (1997) Consensus recommendations for the postmortem diagnosis of Alzheimer's disease. The National Institute on Aging and Reagan Institute Working Group

on diagnostic criteria for the neuropathological assessment of Alzheimer's disease. Neurobiol Aging 18:S1–S2
38. Tolnay M, Schwietert M, Monsch AU, Staehelin HB, Langui D, Probst A (1997) Argyrophilic grain disease: distribution of grains in patients with and without dementia. Acta Neuropathol (Berl) 94:353–358
39. Tolnay M, Mistl C, Ipsen S, Probst A (1998) Argyrophilic grains of Braak: occurrence in dendrites of neurons containing hyperphosphorylated tau protein. Neuropathol Appl Neurobiol 24:53–59
40. Tolnay M, Calhoun M, Pham HC, Egensperger R, Probst A (1999) Low amyloid (Abeta) plaque load and relative predominance of diffuse plaques distinguish argyrophilic grain disease from Alzheimer's disease. Neuropathol Appl Neurobiol 25:295–305
41. Tolnay M, Ghebremedhin E, Probst A, Braak H (2003) Argyrophilic grain disease. In: Dickson D (ed) Neurodegeneration: the molecular pathology of dementia and movement disorders. ISN Neuropathol, Basel, pp 132–136
42. Tsai J, Grutzendler J, Duff K, Gan WB (2004) Fibrillar amyloid deposition leads to local synaptic abnormalities and breakage of neuronal branches. Nat Neurosci 7:1181–1183
43. Van Hoesen G, Pandya DN (1975) Some connections of the entorhinal (area 28) and perirhinal (area 35) cortices of the rhesus monkey. I. Temporal lobe afferents. Brain Res 95:1–24
44. Wu CC, Chawla F, Games D, Rydel RE, Freedman S, Schenk D, Young WG, Morrison JH, Bloom FE (2004) Selective vulnerability of dentate granule cells prior to amyloid deposition in PDAPP mice: digital morphometric analyses. Proc Natl Acad Sci USA 101:7141–7146